



# A release from developmental bias accelerates morphological diversification in butterfly eyespots

Oskar Brattström<sup>a,b,1,2</sup>, Kwaku Aduse-Poku<sup>a,3</sup>, Erik van Bergen<sup>a,4</sup>, Vernon French<sup>c</sup>, and Paul M. Brakefield<sup>a,d</sup>

<sup>a</sup>Department of Zoology, University of Cambridge, CB2 3EJ Cambridge, United Kingdom; <sup>b</sup>African Butterfly Research Institute (ABRI), 0800 Nairobi, Kenya; <sup>c</sup>Institute of Evolutionary Biology, University of Edinburgh, Edinburgh, EH9 3JT, United Kingdom; and <sup>d</sup>Cambridge University Museum of Zoology, CB2 3EJ Cambridge, United Kingdom

Edited by Sean B. Carroll, Howard Hughes Medical Institute, College Park, MD, and approved September 8, 2020 (received for review April 28, 2020)

Development can bias the independent evolution of traits sharing ontogenetic pathways, making certain evolutionary changes less likely. The eyespots commonly found on butterfly wings each have concentric rings of differing colors, and these serially repeated pattern elements have been a focus for evo–devo research. In the butterfly family Nymphalidae, eyespots have been shown to function in startling or deflecting predators and to be involved in sexual selection. Previous work on a model species of *Mycalesina* butterfly, *Bicyclus anynana*, has provided insights into the developmental control of the size and color composition of individual eyespots. Experimental evolution has also shown that the relative size of a pair of eyespots on the same wing surface is highly flexible, whereas they are resistant to diverging in color composition, presumably due to the underlying shared developmental process. This fixed color composition has been considered as a prime example of developmental bias with significant consequences for wing pattern evolution. Here, we test this proposal by surveying eyespots across the whole subtribe of *Mycalesina* butterflies and demonstrate that developmental bias shapes evolutionary diversification except in the genus *Heteropsis* which has gained independent control of eyespot color composition. Experimental manipulations of pupal wings reveal that the bias has been released through a novel regional response of the wing tissue to a conserved patterning signal. Our study demonstrates that development can bias the evolutionary independence of traits, but it also shows how bias can be released through developmental innovations, thus, allowing rapid morphological change, facilitating evolutionary diversification.

evolutionary biology | developmental biology | developmental bias

The developmental mechanisms that generate morphology can, in theory, bias the independent evolution of traits sharing ontogenetic pathways, making certain evolutionary changes less likely than others (1–8). Eyespots are concentric circular markings, often with contrasting colors, that are found on the wings of many Lepidoptera (9–11). In the butterfly family Nymphalidae, a series of similar eyespots is usually displayed toward the margin of the wings. These have been shown to function in startling or deflecting predators (12–15) and to be involved in sexual selection (16, 17). Eyespots have played an important role in the growing research field of evo–devo both because of their simple 2D structure and their rich interspecific diversity in size and color composition (9, 18–21). Surgical damage (22) and grafting (18, 23) experiments on early pupae demonstrated the role of the central focus in producing a signal that induces the surrounding cells to form the differently pigmented scales of an eyespot. Other studies have provided insights into the developmental control of the size and color composition of individual eyespots (10, 20, 24). Experimental evolution using a model species of *Mycalesina* butterfly, *B. anynana*, has also shown that the relative size of eyespots on the same wing surface is highly flexible with little or no bias (25), whereas they are resistant to diverging in color composition, presumably due to the underlying shared developmental process (26).

Together these studies contributed to a model of eyespot formation that, in its simplest form, involves the early pupal focal

cells releasing a signal (e.g., a diffusible morphogen) that spreads out to form a circular concentration gradient (21, 26). The surrounding cells have sensitivity thresholds that direct the color of the pigmented scales that are formed. Below a certain signal threshold, the cells do not respond and will continue to develop into the normal base color of the wing, effectively forming the outer edge of the eyespot. Despite two decades of research gradually unraveling the genetic basis of the developmental processes of butterfly eyespots, the exact nature of the focal signal remains unknown. In Old World tropical butterflies of the Nymphalidae subtribe *Mycalesina* (27) (containing the genus *Bicyclus* and nine other genera), the order of colors typically displayed from the center (high signal level) to the outer (low signal level) ring of a normal eyespot are white, black, and yellow–gold–orange (subsequently called yellow) (Fig. 1). By changing the signal level produced by each focus, the size of the individual eyespots can be modified, however, it seems that the signal thresholds for the different color transitions may be fixed across the whole surface of each wing, explaining why relative proportions cannot be modulated at the level of individual eyespots (26). This has been considered as a prime example of developmental bias with significant consequences for wing pattern evolution (26).

## Significance

The concept of developmental bias argues that developmental processes can influence the direction of evolutionary change in morphology. We survey wing patterns across *Mycalesina* butterflies, focusing on a pattern element called eyespots. The relative color composition of these spots has been considered to be a prime example of developmental bias but had not been studied extensively in a phylogenetic context. We show that developmental bias is limiting the evolutionary independence of eyespot color composition but not size in most groups of *Mycalesina* butterflies. However, a release from developmental bias has enabled the Malagasy genus *Heteropsis* to evolve more diverse wing patterns. Using laboratory experiments, we investigate the developmental changes underlying this release.

Author contributions: O.B., V.F., and P.M.B. designed research; O.B. and K.A.-P. performed research; O.B., K.A.-P., and E.v.B. analyzed data; and O.B., V.F., and P.M.B. wrote the paper.

The authors declare no competing interest.

This article is a PNAS Direct Submission.

Published under the PNAS license.

<sup>1</sup>To whom correspondence may be addressed. Email: oskar.brattstrom@gmail.com.

<sup>2</sup>Present address: University of the West of Scotland, Paisley Campus, Paisley, PA1 2BE, Scotland, United Kingdom.

<sup>3</sup>Present address: Georgia State University, Perimeter College, Life & Earth Sciences Department, Decatur, GA 30034.

<sup>4</sup>Present address: Research Centre for Ecological Change, Organismal and Evolutionary Biology Research Programme, Faculty of Biological and Environmental Sciences, University of Helsinki, FI-00014 Helsinki, Finland.

This article contains supporting information online at <https://www.pnas.org/lookup/suppl/doi:10.1073/pnas.2008253117/-DCSupplemental>.

First published October 22, 2020.

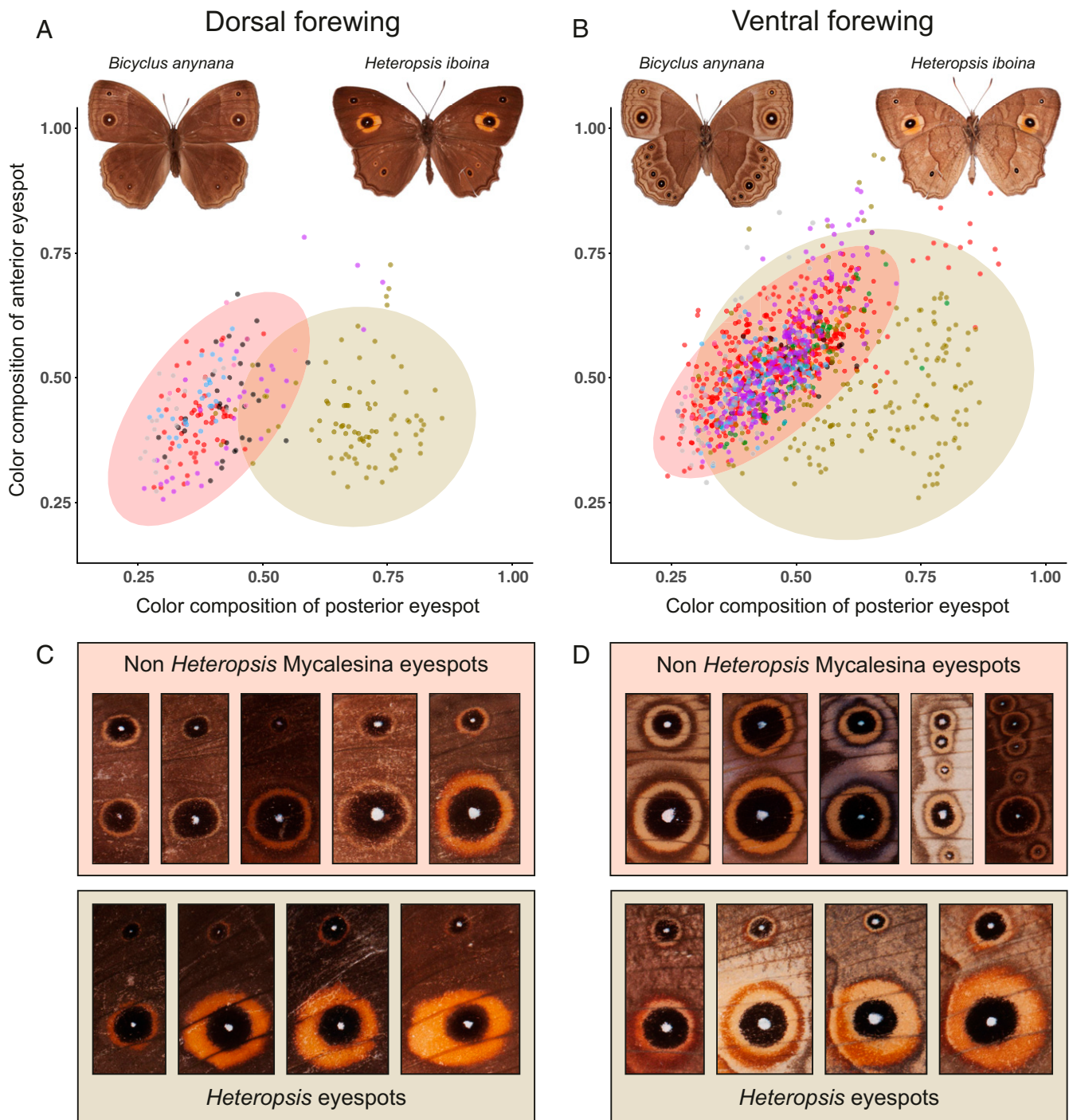


**Fig. 1.** Color compositions of dorsal and ventral forewing eyespots. Correlation of the color composition—the proportion of the total eyespot area covered by yellow scales—between the anterior (cell  $M_1$ ) and the posterior (cell  $CuA_1$ ) eyespots on the forewings of *Mycalesina* butterflies as measured from 1,249 male specimens from 288 taxa. The samples from different genera are color coded following the color scheme from Fig. 2 with each dot representing an individual specimen. Computed normal confidence ellipses highlight the wide exploration of morphospace for the Malagasy genus *Heteropsis* (light olive). In contrast, the eyespot color compositions in the other genera (light red) are strongly correlated, supporting the presence of developmental bias. Data for both (A) dorsal and (B) ventral wing surfaces only include specimens that possess both of the investigated eyespots with both having yellow rings. (C and D) show examples of eyespots from species in the two color-coded groups shown in A and B. (C) Dorsal eyespots in Top (Left to Right): *Bicyclus jacksoni*, *Telinga misenus*, *Mydosama asophis*, *Mycalesis madjicosa*, and *Brakefieldia perspicua*. Dorsal eyespots in Lower: *Heteropsis angulifascia*, *Heteropsis pauper*, *Heteropsis ankova*, and *Heteropsis turbans*. (D) Ventral eyespots in Top: *Lohora dexamenus*, *Mydosama duponchelii*, *Bicyclus rileyi*, *Hallelesis halyma*, and *Culapa kina*. Ventral eyespots in Lower: *Heteropsis ankaratra*, *Heteropsis fraterna*, *Heteropsis strigula*, and *Heteropsis turbata*.

A study investigating eyespots across a large number of *Mycalesina* species found that, with regard to their total size, there seems to be no strong bias limiting the independence of the main dorsal forewing

eyespots (28), just as indicated by the selection experiment in *B. anynana* (24). However, to date, the question of the extent of bias in eyespot color composition across *Mycalesina* has not been addressed.

## Results and Discussion

Based on a multigene phylogeny containing over 80% of the described species of Mycalesina, we measured the size of separate color elements of the two main forewing eyespots from multiple male specimens from taxa for which we also had phylogenetic information. We deliberately focused on the male patterns as females of some species can be difficult to identify. The patterns in the relative size of the forewing eyespots showed no evidence of any strong bias limiting the independence of the main dorsal forewing eyespots (*SI Appendix, Fig. S1*) which is consistent with previous studies in *B. anynana* (24, 28). We, then, calculated the color composition, defined as the relative proportion of the total eyespot area formed by the outer ring of yellow scales in the two main eyespots on both dorsal and ventral forewing surfaces. There was a tight correlation between the color composition of the two eyespots in most sampled specimens, consistent with a developmental bias limiting the independent evolution of eyespot color composition. However, the majority of species in the Malagasy genus *Heteropsis* show greatly increased yellow rings in the posterior but not the anterior eyespot (Fig. 1), suggesting a release from the bias within this lineage.

To be able to study the correlation of eyespot color composition in detail, we calculated an index of eyespot similarity (ES) with regard to the color composition (see *Methods* for details) between the two main eyespots on each surface of the forewing. An ES ratio of 1 reflects that the color compositions of the two eyespots are equal, while any deviation from 1 indicates within-surface variation in eyespot color composition. Using variable-rates models in the software Bayes Traits V3.0.1 (29), we estimated the ancestral states of the eyespot similarity and reconstructed historical shifts in the speed of morphological changes across the phylogeny. These analyses showed a marked increase in morphological evolution early in the genus *Heteropsis* with only the first basal clade behaving, like most other Mycalesina, in showing very little evidence for significantly increased rates of evolution (Fig. 2 and *SI Appendix, Fig. S2*). The topology of the tree itself shows that there has been a release from the bias and not just a shift to a new fixed proportion between eyespots as the latter would have resulted in a tree with a single long branch

leading up to a renewed slowly evolving phase of relative stasis (30). Once the bias is removed, active natural selection for specific morphologies as well as neutral drift is expected to keep the ratio between the two eyespots in a state of dynamic change as long as strong stabilizing selection is not acting against it.

To investigate the developmental basis of the enlarged yellow elements of the posterior eyespots of *Heteropsis*, we performed surgical grafts on developing pupae of the species *Heteropsis iboina*. These involved moving the focal cells from the large posterior eyespot into five more anterior host positions (Fig. 3A). This was performed to investigate whether the enlarged yellow ring of the posterior eyespot resulted from the nature of the posterior focal signal or from different response thresholds in the anterior and posterior parts of the wing. The results from 473 grafted pupae reveal that the posterior focal signal forms an ectopic eyespot with a narrow yellow ring when positioned anteriorly but with a broader yellow region when it extends more posteriorly on the wing (Fig. 3B–G). This demonstrates that the evolutionary change that broke the linkage between eyespots has happened by modulating the response of the posterior tissue to an unchanged focal signal. Detailed inspection of the resulting wings suggested that there is a sharp border on the wing around the region of vein  $M_3$  with the yellow scales reaching much further down toward the posterior part of the wing once the focal signal had crossed the vein (Fig. 3D and E). Smaller ectopic eyespots where the focal signal did not cross vein  $M_3$  looked like the normal anterior eyespot (in wing cell  $M_1$ ) with a narrow outer yellow ring (Fig. 3F). The effect was analyzed by calculating the ratio of the posterior width of the yellow ring divided by its distal width: this ratio was significantly higher for eyespots that crossed over vein  $M_3$  (Fig. 3H).

On the experimental wings, the ectopic eyespot induced around the grafted focus was usually considerably smaller than the normal posterior eyespot, and a prominent yellow (or black and yellow) pattern was frequently formed in that  $CuA_1$  wing cell, despite the removal of the focus when grafting the wing (Fig. 3G). It is likely that these effects arise from focal signaling starting at (or even before) the time of pupation (18, 23) and, therefore, before the time of grafting. However, it was not possible to perform surgical operations on very early pupae as the cuticle needs to somewhat

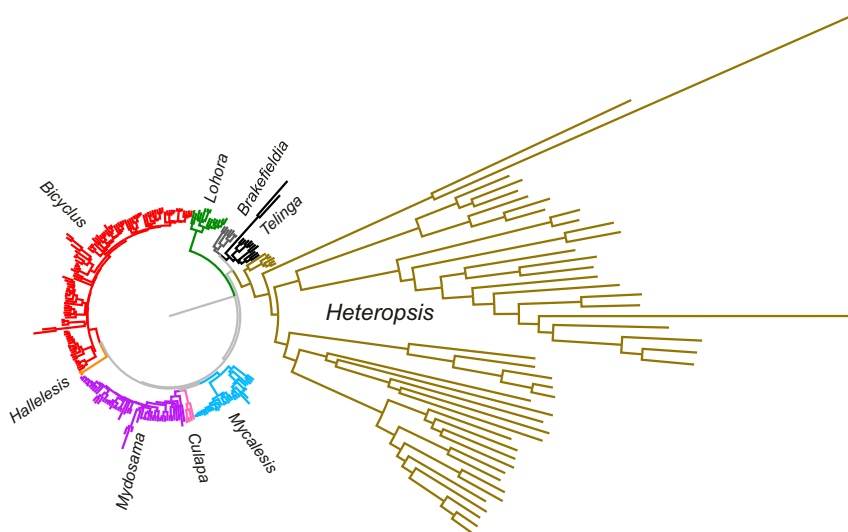


**Fig. 2.** Variable rates of evolution in eyespot similarity across the Mycalesina phylogeny. Estimated historical rate of morphological evolution in eyespot similarity—the difference in color composition of the two main eyespots—on the ventral wing surface. All branches of the Mycalesina phylogeny are scaled by the amount of morphological change estimated by the variable-rates model (Bayes Traits V3.0.1). Branches with high rates of morphological change are extended, while those with low rates are compressed. Continued acceleration of morphological diversification is observed in the genus *Heteropsis*, starting around the time of the first basal branching event, resulting in a wider exploration of morphospace (Fig. 1). The reconstruction of eyespot similarity on the dorsal forewing surface shows a similar pattern (*SI Appendix, Fig. S2*).

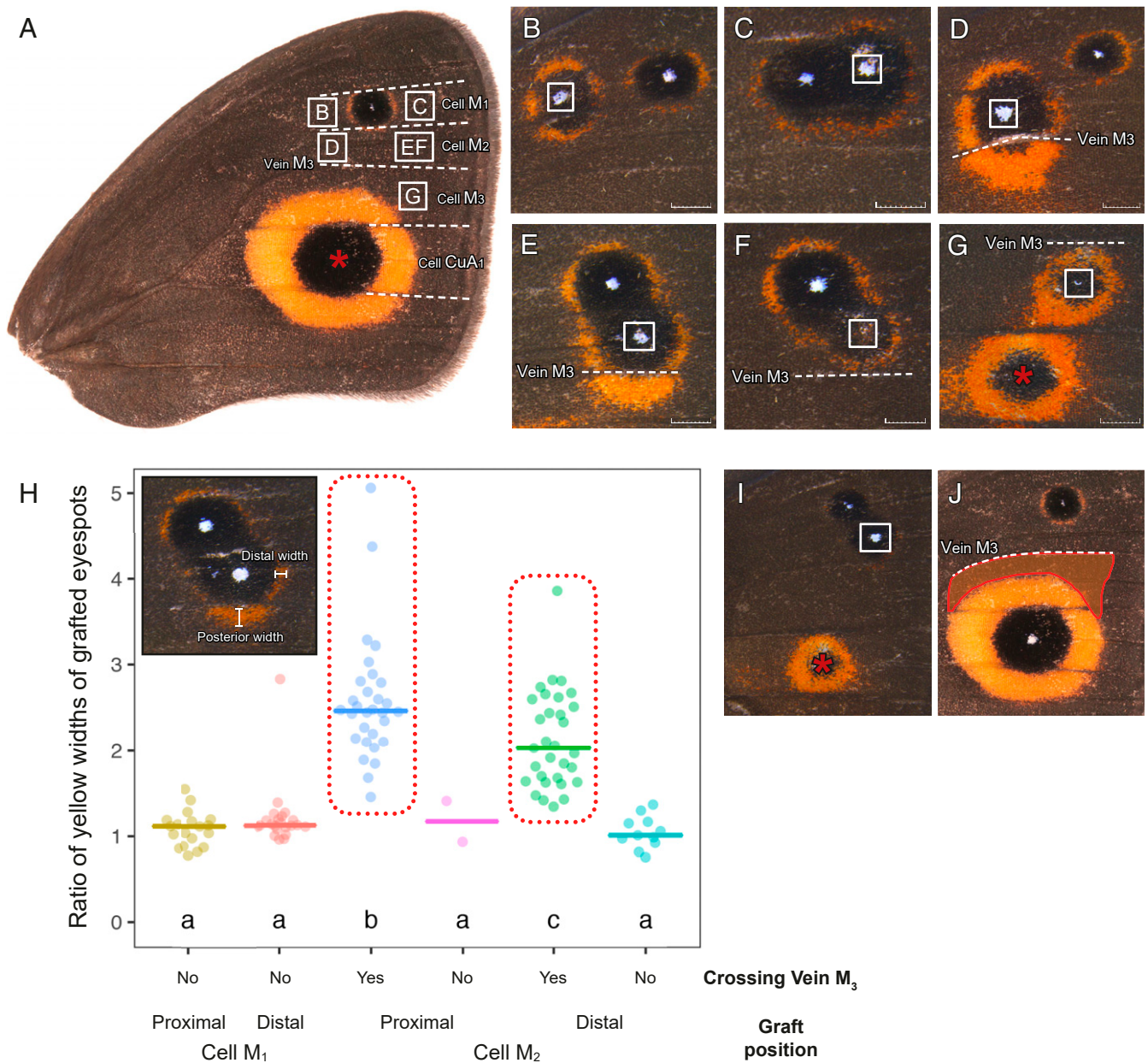


**Fig. 3.** Results of grafting experiments. (A) The developmental basis of the enlarged yellow ring of *Heteropsis* was studied by performing surgical manipulations on pupal wings from the Malagasy butterfly *H. iboina* (normal dorsal forewing depicted). Ectopic eyespots were induced by grafting the dorsal posterior focal cells from wing cell CuA<sub>1</sub> (red asterisk) into three distal and two proximal donor positions on the anterior wing (white squares). Grafts moved into a proximal (B) or distal (C) position in wing cell M<sub>1</sub>—next to the normal anterior focus—induce an ectopic eyespot with a narrow yellow ring. Grafts moved into a proximal (D) or distal (E and F) position in wing cell M<sub>2</sub> induce an ectopic eyespot with a narrow yellow ring that expands posteriorly when the focal signal crosses vein M<sub>3</sub> (D and E). Grafts moved into a distal (G) position in wing cell M<sub>3</sub> induce an ectopic eyespot with an enlarged yellow ring that typically fuses with a (reduced) posterior eyespot formed in wing cell CuA<sub>1</sub> (see the main text). Scale bars correspond to 1 mm. (H) Comparison of the ratios of the posterior and distal widths of yellow in ectopic eyespots around the grafted foci showed a significant difference between eyespots crossing over vein M<sub>3</sub>, compared to those which did not (significant differences between groups [see *Methods*] are indicated by different letters). (I) Grafting frequently resulted in a marked reduction of patterning from the area around where the graft was taken from. (J) Ectopic eyespots form enlarged yellow rings within a region that is well outside the yellow area of an unmanipulated posterior eyespot (shown by the overlay).

harden to avoid the pupae collapsing during surgery. The residual CuA<sub>1</sub> pattern was frequently strongly reduced or almost absent (Fig. 3J), showing that the broad yellow ring is, indeed, the outer element of the posterior eyespot as patterned by the focal signal (rather than being a separate novel pattern element). Further evidence comes from the fact that ectopic patterns induced by grafts placed in cell M<sub>2</sub> (and crossing over into cell M<sub>3</sub>) as well as grafts placed in cell M<sub>3</sub> consistently produce extensive yellow

scales in an upper region of cell M<sub>3</sub> that is typically uniformly brown (Fig. 3J). In other words, if the posterior pattern were formed by a typical *Mycalesina* eyespot superimposed on a large yellow patch, ectopic eyespots around a grafted focus should only form narrow yellow rings in all other regions of the wing.

Our results from tissue transplantations suggest various ways in which the novel eyespot morphology in the *Heteropsis* lineage may have arisen at the genetic level. Eyespot patterning is not

fully understood, but there is evidence of the involvement of the Wingless, Hedgehog, Notch signaling pathways, and of transcription factors including Distal-less, Engrailed, Spalt, and Antennapedia (31–33). Also, butterfly larval imaginal disks, like those of *Drosophila*, express certain genes (e.g., *engrailed* and *Apterous*) only in specific wing regions, and these could act as selector genes, modulating patterning within the eyespots developing in different locations (21). It has been suggested that the uniformity in eyespot color composition typical of species of *Mycaliesina* results from this feature being specified after the phase of region-specific gene expression (21). The novelty in the *Heteropsis* wing pattern that is reflected in the differently proportioned eyespots developed by the anterior and posterior wing cells in response to focal signaling may have resulted from changes in the extent or timing of the expression of selector genes in late larval imaginal disks or from changes in the input that particular selector genes have into the processes of eyespot patterning. In either of these ways, the response to focal signaling may have become dependent on the region-specific expression of selector genes, distinguishing anterior from posterior wing regions in the level at which yellow fate changes to the background brown color, thus, setting different widths of the outer ring of their eyespots. It is intriguing that the particular region around vein  $M_3$  (which is distant from the anterior–posterior compartment border) has recently been suggested to also be of developmental significance in the wings of other Lepidopteran insects (34). A fuller understanding and experimental manipulation of the region-specific selector genes will be needed to reveal the genetic basis of the novel phenotype, but having identified a border on the wing with a strong effect on the response to the focal signal will make it easier to detect candidate genes by comparisons of gene expression data from different wing regions. It would also be valuable to establish new laboratory colonies of further species of *Mycaliesina* specifically selected for their eyespot morphology and position in the phylogeny. Key targets would be species in the small clade of *Heteropsis* that show no evidence of having been released from bias. Using stocks from such species for further grafting work and artificial selection experiments similar to those performed on *B. anynana* (10, 25, 26) would provide vital data to understand, in detail, how developmental bias have influenced the evolution of eyespots in *Mycaliesina*.

Taken together, our results show that the color composition of the eyespots of most species of *Mycaliesina* are strongly correlated and have little flexibility in their individual evolutionary options. This suggests that covariation through shared development can contribute to shaping diversification, but on a macroevolutionary scale such bias can be broken and enable rapid exploration of previously inaccessible parts of morphospace as demonstrated here by the genus *Heteropsis*. In the field, as well as in free-flying greenhouse populations, *Heteropsis* butterflies exhibit a ritualized display of rapidly opening and closing their wings on alighting, thus, exposing the conspicuous dorsal eyespot to startle a potential predator. This contrasts with the primarily deflective role of eyespots in other genera (15, 35) and suggests that the novel morphology, in combination with co-option of deimatic behavior, has facilitated evolutionary diversification in the Malagasy clade. Our results emphasize that understanding how development can bias available variation in morphology can make a valuable contribution to explaining and predicting patterns of evolutionary diversification. Essentially, we now have an example where the demonstration of the potential for developmental bias in a model species has been extended to show how this is reflected in species-rich parallel radiations. In addition, we have shown that a pattern of bias, rather than a strict developmental constraint, can be released by a developmental innovation to result in a spectacular radiation in to novel phenotypic space.

## Materials and Methods

**Phylogeny Construction.** Some 303 taxa representing all known genera of *Mycaliesina* (*Bicyclus*, *Brakefieldia*, *Culapa*, *Devyatkinia*, *Hallelesis*, *Heteropsis*, *Lohora*, *Mycaliesis*, *Mydosama*, and *Telinga*) were included as the exemplar taxa for this study. Additionally, eight taxa of the *Lethina* subtribe were included as outgroups. Genomic DNA was extracted from abdomens or legs using a Qiagen DNEasy extraction kit following the manufacturer's protocol. A total of 10 protein-coding molecular markers were amplified and sequenced: One mitochondrial (cytochrome c oxidase subunit I, *COI*) and nine nuclear (carbamoylphosphate synthetase domain protein, *CAD*; ribosomal protein S5, *RpS5*; ribosomal protein S2, *RpS2*; wingless, *wg*; cytosolic malate dehydrogenase, *MDH*; glyceraldehyde-3-phosphate dehydrogenase, *GAPDH*; elongation factor 1  $\alpha$ , *EF-1 $\alpha$* ; arginine kinase, *ArgKin*; and isocitrate dehydrogenase, *IDH*) gene regions were amplified. DNA amplification and sequencing followed the methodology of Aduse-Poku et al. (36). Sequences and voucher specimens for the phylogenetic work were primarily obtained from previously published studies of *Mycaliesina* butterflies (27, 36–42) with some new sequences procured from field work and museum collections. A complete list of all voucher specimen data and accession codes are available in [Dataset S1](#). We reconstructed our phylogenies using both maximum likelihood (ML) and Bayesian inference (BI) methods. The ML analysis was performed in IQ-TREE v.1.6.3 (43) using the best partitioning scheme and best models of nucleotide substitution suggested by ModelFinder (44). The dataset was divided a priori by codon positions, resulting in 30 partitions. We estimated simultaneously the BI tree and divergence times using BEAST 1.8.4 (45). The best partitioning scheme and models of substitution for the Bayesian analyses were estimated in PartitionFinder2 (46). Given the recent controversy on Lepidoptera fossils (47), we used a more recent extensive fossil-based dating framework (48) for our dating analysis. Consequently, we constrained the node corresponding to the divergence between *Lethina* and *Mycaliesina* with a uniform prior encompassing the 95% credibility interval (25.1–44.1 Ma) estimated for this node (48). All analyses consisted of 50 million generations with a parameter and tree sampling every 5,000 generations.

**Taxonomic Nomenclature.** References to homologous wing veins and cells follow the system proposed by R.J. Wootton (49).

**Museum Specimens.** An extensive data set of images was assembled by photographing specimens from 10 museums and three private collections ([SI Appendix, Table S1](#)). For taxa for which phylogenetic data were available, we aimed to include, at least, five specimens in measurable condition. We focused on male specimens to prevent misidentification of taxa—females of some *Mycaliesina* butterflies cannot be identified to species level without dissection or genetic testing (50). Seasonal polyphenism is prevalent in this group of butterflies (51, 52), and to exclude the effect of developmental plasticity (i.e., high intraspecific variation in eyespot size and color composition, [SI Appendix, Fig. S3](#)), we focused on specimens that showed full expression of the wet season from phenotype, avoiding aberrant males with extreme eyespot phenotypes. The excluded specimens all showed a marked increase in the amount of yellow around their eyespots (similar to the previously documented mutations in *B. anynana*, such as Goldeneye (20), and since these enlarged eyespots typically merge with neighboring eyespots, they could not be measured in a repeatable way. Both this aberration and the seasonal variation affected all eyespots equally as expected from developmental bias. For nine exceedingly rare taxa, or ones not as yet fully described, we were not able to find suitable male specimens, and six additional species were excluded because homology of color pattern elements could not be inferred with certainty. The final data set included 1,249 images from 288 taxa ([SI Appendix, Table S2](#)).

**Image Acquisition.** The majority of the specimens (98.3%) were photographed using a Nikon D300 SLR with an AF-S Micro NIKKOR 60 mm f/2.8G ED lens set at a fixed focus distance of 7, 9, or 10 cm. Lighting was provided by using a Metz Ring Flash 15 MS-1, and all exposure settings—including flash output—were locked to predetermined settings to ensure comparative images. Captured RAW files were developed in Adobe Photoshop CC 2018 with fixed settings. Colors and contrasts were balanced using QPcolorsoft 501 software (2.0.1.) and reference images of a QP Card 201 that were acquired using the same procedure as for specimens. The remaining 21 specimens were analyzed from a range of photographs taken with various cameras but with a reliable scale included in the image such that size could be correctly measured.

**Image Analyses.** Images were analyzed using custom-made macros and the image processing package Fiji 1.0 (53) coupled to ImageJ 1.51 (54). Two

different areas of each of the eyespots in cells CuA<sub>1</sub> and M<sub>1</sub> were quantified as freehand selections using a pen monitor (Huion Kamvas GT-220) to enable accurate marking of fine details. The eyespots on both the dorsal and the ventral surfaces of the forewing were included. We measured the total area of the complete eyespot including the combined areas of the central focus, black inner disk, and the yellow outer ring. We also measured the combined area of the central focus and the black inner disk to be able to calculate the total and relative area of the eyespots' yellow ring. The straight-line distance between the end points of vein CuA<sub>2</sub> was quantified and used as a proxy for wing size (see below). Using this approach, all raw data values could be measured with high repeatability ( $R^2 > 0.99$ ), and the variables that were derived from further calculations using the raw data also showed a high repeatability ( $R^2 = 0.99\text{--}0.81$ ). A summary of all repeatability tests is shown in *SI Appendix, Table S3*. Raw data from the image analyses are available in *Dataset S1*.

**Data Transformation for Surface-Specific Analyses.** We calculated the relative eyespot size by dividing the total eyespot area by the squared wing index (see above). This allowed us to visually inspect our data on eyespot sizes and to compare them to previously published data (28) (*SI Appendix, Fig. S1*). The color composition of each eyespot was defined as the relative proportion covered by yellow–gold–orange scales (i.e., the outer ring) and was calculated by dividing the yellow area by the total area. The relationships between the color composition and the relative size of the eyespots were visualized using the package *ggplot2* (55) in R (56). For each individual, ES was assessed by dividing the color composition of the largest eyespot by that of the smallest eyespot on the same wing surface. Hence, an ES ratio of 1 reflects that the color compositions of the two eyespots are equal, while any deviation from 1 indicates within-surface variation in eyespot color composition. Taxa possessing only one eyespot on the forewing, which is typical for the dorsal surface in some genera, or those that had eyespots that did not show an outer yellow ring, were excluded from further surface-specific analyses. After excluding 12 taxa that had only a single or no spot with yellow scales on either wing surface, our total data set for eyespot color composition comprised 76 and 273 taxa for the dorsal and ventral surfaces, respectively. The eyespot in cell CuA<sub>1</sub> was the largest eyespot for all species included in the dorsal analyses and for all but nine of the species included in the ventral analyses.

**Evolutionary Analyses.** To detect shifts in the rate of ES across the phylogeny, we used the variable-rates model described by Baker et al. (30) as implemented in the software package BayesTraits V3.0.1 (29) (available at [www.evolution.rdg.ac.uk](http://www.evolution.rdg.ac.uk)). All analyses were conducted using the time-calibrated, multigene consensus tree, and mean ES per taxon as the focal trait. Reversible-jump Markov chain Monte Carlo algorithms were run for 105 million iterations with a burn-in period of 5 million generations after which the chain was sampled every 100,000th iteration. Priors were kept at default for all analyses, and each run was repeated five times to confirm the stability of the logarithmic marginal likelihoods and to check the topologies of the consensus trees. The logarithmic marginal likelihoods for the  $m_0$  (fixed-rates) and  $m_1$  (variable-rates) models were estimated using stepping-stone sampling implemented in BayesTraits and then used to compute a logarithmic Bayes factor (BF). We ran the stepping-stone sampler with 1,000 stones and 100,000 iterations for each stone following the completion of each analysis. BFs were used as the test statistic; values greater than 2 are typically considered positive evidence, and BFs greater than 10 are taken as very strong evidence for rate variation (57). We found strong support for variable rates of morphological changes on both wing surfaces (ventral,  $BF_{\text{mean}} = 160.4$ ; dorsal,  $BF_{\text{mean}} = 22.6$ ; *SI Appendix, Table S4*). The variable-rates model identified increased rates of evolution as mainly occurring along the branches of the *Heteropsis* clade (Fig. 2 and *SI Appendix, Fig. S2*), strongly implying that these species have gained independent control of eyespot color composition. Input data for the evolutionary analyses are available in *Dataset S1*.

**Grafting Experiment.** Larvae from a laboratory population of *H. iboina* (58) were reared on basketgrass (*Oplismenus compositus*) in climate-controlled chambers (Panasonic MLR-352H-PE) at 25 °C, 75% relative humidity, and a 12:12 light:dark cycle. Prepupae were collected daily and placed in compartmentalized Petri dishes. Using time-lapse photography, we recorded the time of pupation to the nearest 15 min. Grafting operations were performed on the dorsal surface of the forewing, 4 to 5 h after pupation when the pupal cuticle had hardened sufficiently to allow surgery but before the underlying wing epidermis had separated. The grafting experiment followed procedures as previously described for *B. anynana* (22). We performed five surgical manipulations, all involving moving a square portion of cuticle with a similar width as the diameter of the circular eyespot focus located in cell CuA<sub>1</sub> (which is easy to locate on the pupal epidermis) to a new host site on the same wing. The tissue removed from the host site was then used to cover the focal area that was used as donor tissue. The five host sites included three distal (in relation to the location of the eyespot in cell M<sub>1</sub>) positions in cells M<sub>1</sub>, M<sub>2</sub>, and M<sub>3</sub>, as well as two proximal locations in cells M<sub>1</sub> and M<sub>2</sub> (see Fig. 3 in the main text). The grafts were performed by first piercing the cuticle at each corner of the planned square graft using a tungsten microneedle with a 1 μm tip. The graft was then carefully cut out using knives made from broken chips of razor blades mounted on a needle holder. The premade holes at the end of each cut help to ensure that the fragile cuticle does not split beyond the extent of the planned cuts. Once the square pieces of cuticle at both the host and the donor sites were fully cut out, a microforceps (Dumont no. 55) was used to quickly swap the pieces of cuticle (and the attached underlying epidermis) between the two sites. After grafting, pupae were left untouched for 30 min to allow the hemolymph to seal the incision sites. Subsequently, pupae were placed in individual transparent pots and returned to the climate-controlled chambers to complete development. One day after eclosion, the adults were frozen to –18 °C after which the wings were removed using surgical scissors. The dorsal surface of the experimental wings was photographed using a Leica DFC495 digital camera coupled to a Leica M125 stereomicroscope. The numbers of performed grafts and associated eclosion rates are presented in *SI Appendix, Table S5*. Images were inspected by eye to assess the effect of the grafting procedure. To estimate the effect of grafts crossing vein M<sub>3</sub> we measured the distal and posterior widths of ectopic eyespots showing clear yellow outlines in grafts placed in cells M<sub>1</sub> and M<sub>2</sub> ( $n = 115$ ). A ratio was calculated for each eyespot by dividing the posterior width by the distal width. These ratios were used as the dependent variable in a linear model with the graft position and the crossing of the vein as a concatenated fixed factor (Fig. 3H). Post hoc pairwise comparisons (Tukey's honestly significant difference;  $\alpha = 0.05$ ) were performed using the *emmeans* package (59).

**Data Availability.** Raw data from the image analyses, input data for the evolutionary analyses, and information on all voucher specimens used in the phylogeny are available as *Dataset S1*. The phylogenetic consensus tree used for the evolutionary analyses is available as *Dataset S2*. DNA sequences have been deposited in GenBank, <https://www.ncbi.nlm.nih.gov/genbank>; all accession numbers are listed in *Dataset S1*. Images of grafted specimens have been deposited in Apollo, <https://doi.org/10.17863/CAM.58236>. All other study data are included in the article and supporting information.

**ACKNOWLEDGMENTS.** Photographs of analyzed specimens were taken from the museum collections of ABRI (Nairobi), MGCL (Gainesville), MNHB (Berlin), MRAC (Tervuren), NHMUK (London), NHMW (Vienna), NHRs (Stockholm), OUMNH (Oxford), NBNC (Leiden), SMNS (Stuttgart), and the personal research collections of Oskar Brattström, Peter Roos, and Robert Tropek. We thank all the Curators and the Trustees of these collections. Rob Freckleton and Michael Akam provided comments on the manuscript. Elishia Harji assisted with proof-reading and language editing. Simon Chen photographed specimens from the collections at SMNS. This work was funded by grants from the John Templeton Foundation (60501) and the European Research Council (EMARES 250325) to P.M.B.

- J. Maynard Smith et al., Developmental constraints and evolution. *Q. Rev. Biol.* **60**, 265–287 (1985).
- W. Arthur, Developmental drive: An important determinant of the direction of phenotypic evolution. *Evol. Dev.* **3**, 271–278 (2001).
- P. M. Brakefield, Evo-devo and constraints on selection. *Trends Ecol. Evol. (Amst.)* **21**, 362–368 (2006).
- K. D. Kavanagh, A. R. Evans, J. Jernvall, Predicting evolutionary patterns of mammalian teeth from development. *Nature* **449**, 427–432 (2007).
- J. A. Fritz et al., Shared developmental programme strongly constrains beak shape diversity in songbirds. *Nat. Commun.* **5**, 3700 (2014).
- C. A. Wessinger, L. C. Hileman, Accessibility, constraint, and repetition in adaptive floral evolution. *Dev. Biol.* **419**, 175–183 (2016).
- T. Uller, A. P. Moczek, R. A. Watson, P. M. Brakefield, K. N. Laland, Developmental bias and evolution: A regulatory network perspective. *Genetics* **209**, 949–966 (2018).
- D. Jablonski, Developmental bias, macroevolution, and the fossil record. *Evol. Dev.* **22**, 103–125 (2020).
- H. F. Nijhout, *The Development and Evolution of Butterfly Wing Patterns*, (Smithsonian Institution Press, Washington, DC, 1991).
- A. F. Monteiro, P. M. Brakefield, V. French, The evolutionary genetics and developmental basis of wing pattern variation in the butterfly *Bicyclus anynana*. *Evolution* **48**, 1147–1157 (1994).
- P. Beldade, P. M. Brakefield, The genetics and evo-devo of butterfly wing patterns. *Nat. Rev. Genet.* **3**, 442–452 (2002).

12. A. D. Blest, The function of eyespot patterns in the Lepidoptera. *Behaviour* **11**, 209–225 (1957).
13. A. Vallin, S. Jakobsson, J. Lind, C. Wiklund, Prey survival by predator intimidation: An experimental study of peacock butterfly defence against blue tits. *Proc. Biol. Sci.* **272**, 1203–1207 (2005).
14. U. Kodandaramaiah, The evolutionary significance of butterfly eyespots. *Behav. Ecol.* **22**, 1264–1271 (2011).
15. K. L. Prudic, A. M. Stoehr, B. R. Wasik, A. Monteiro, Eyespots deflect predator attack increasing fitness and promoting the evolution of phenotypic plasticity. *Proc. Biol. Sci.* **282**, 20141531 (2015).
16. C. J. Breuker, P. M. Brakefield, Female choice depends on size but not symmetry of dorsal eyespots in the butterfly *Bicyclus anynana*. *Proc. Biol. Sci.* **269**, 1233–1239 (2002).
17. K. L. Prudic, C. Jeon, H. Cao, A. Monteiro, Developmental plasticity in sexual roles of butterfly species drives mutual sexual ornamentation. *Science* **331**, 73–75 (2011).
18. H. F. Nijhout, Pattern formation on lepidopteran wings: Determination of an eyespot. *Dev. Biol.* **80**, 267–274 (1980).
19. P. M. Brakefield *et al.*, Development, plasticity and evolution of butterfly eyespot patterns. *Nature* **384**, 236–242 (1996).
20. C. R. Brunetti *et al.*, The generation and diversification of butterfly eyespot color patterns. *Curr. Biol.* **11**, 1578–1585 (2001).
21. A. Monteiro, Origin, development, and evolution of butterfly eyespots. *Annu. Rev. Entomol.* **60**, 253–271 (2015).
22. V. French, P. M. Brakefield, The development of eyespot patterns on butterfly wings: Morphogen sources or sinks? *Development* **116**, 103–109 (1992).
23. V. French, P. M. Brakefield, Eyespot development on butterfly wings: The focal signal. *Dev. Biol.* **168**, 112–123 (1995).
24. A. Monteiro, P. M. Brakefield, V. French, Butterfly eyespots: The genetics and development of the color rings. *Evolution* **51**, 1207–1216 (1997).
25. P. Beldade, K. Koops, P. M. Brakefield, Developmental constraints versus flexibility in morphological evolution. *Nature* **416**, 844–847 (2002).
26. C. E. Allen, P. Beldade, B. J. Zwaan, P. M. Brakefield, Differences in the selection response of serially repeated color pattern characters: Standing variation, development, and evolution. *BMC Evol. Biol.* **8**, 94 (2008).
27. K. Aduse-Poku *et al.*, Systematics and historical biogeography of the old world butterfly subtribe Mycalesina (Lepidoptera: Nymphalidae: Satyrinae). *BMC Evol. Biol.* **15**, 167 (2015).
28. P. M. Brakefield, J. C. Roskam, Exploring evolutionary constraints is a task for an integrative evolutionary biology. *Am. Nat.* **168**, S4–S13 (2006).
29. A. Meade, M. Pagel, BayesTraits V3.0.1. [www.evolution.rdg.ac.uk/BayesTraitsV3.0.1/BayesTraitsV3.0.1.html](http://www.evolution.rdg.ac.uk/BayesTraitsV3.0.1/BayesTraitsV3.0.1.html). (2017). Accessed 23 November 2017.
30. J. Baker, A. Meade, M. Pagel, C. Venditti, Positive phenotypic selection inferred from phylogenies. *Biol. J. Linn. Soc. Lond.* **118**, 95–115 (2016).
31. H. Connahs *et al.*, Activation of butterfly eyespots by Distal-less is consistent with a reaction-diffusion process. *Development* **146**, 169367 (2019).
32. L. Zhang, R. D. Reed, Genome editing in butterflies reveals that spalt promotes and Distal-less represses eyespot colour patterns. *Nat. Commun.* **7**, 11769 (2016).
33. L. Livraghi *et al.*, CRISPR/Cas9 as the key to unlocking the secrets of butterfly wing pattern development and its evolution. *Adv. Insect Physiol.* **54**, 85–115 (2017).
34. R. Abbasi, J. M. Marcus, A new A-P compartment boundary and organizer in holometabolous insect wings. *Sci. Rep.* **7**, 16337 (2017).
35. A. Lyytinen, P. M. Brakefield, J. Mappes, Significance of butterfly eyespots as an anti-predator device in ground-based and aerial attacks. *Oikos* **100**, 373–379 (2003).
36. K. Aduse-Poku *et al.*, Molecular phylogeny and generic-level taxonomy of the widespread palaeotropical ‘*Heteropsis* clade’ (Nymphalidae: Satyrinae: Mycalesina). *Syst. Entomol.* **41**, 717–731 (2016).
37. A. Monteiro, N. E. Pierce, Phylogeny of *Bicyclus* (Lepidoptera: Nymphalidae) inferred from COI, COII, and EF-1 $\alpha$  gene sequences. *Mol. Phylogenet. Evol.* **18**, 264–281 (2001).
38. D. Murray, D. P. Prowell, Molecular phylogenetics and evolutionary history of the neotropical satyrine subtribe euptychiina (Nymphalidae: Satyrinae). *Mol. Phylogenet. Evol.* **34**, 67–80 (2005).
39. C. Peña *et al.*, Higher level phylogeny of Satyrinae butterflies (Lepidoptera: Nymphalidae) based on DNA sequence data. *Mol. Phylogenet. Evol.* **40**, 29–49 (2006).
40. C. Peña, N. Wahlberg, Prehistorical climate change increased diversification of a group of butterflies. *Biol. Lett.* **4**, 274–278 (2008).
41. C. Peña, S. Nylin, N. Wahlberg, The radiation of satyrini butterflies (Nymphalidae: Satyrinae): A challenge for phylogenetic methods. *Zool. J. Linn. Soc.* **161**, 64–87 (2011).
42. S. Osozawa, M. Takahashi, J. Wakabayashi, Ryukyu endemic *Mycalesis* butterflies, speciated vicariantly due to isolation of the islands since 1.55 Ma. *Lepid. Sci.* **66**, 8–14 (2015).
43. L. T. Nguyen, H. A. Schmidt, A. von Haeseler, B. Q. Minh, IQ-TREE: A fast and effective stochastic algorithm for estimating maximum-likelihood phylogenies. *Mol. Biol. Evol.* **32**, 268–274 (2015).
44. S. Kalyaanamoorthy, B. Q. Minh, T. K. F. Wong, A. von Haeseler, L. S. Jermini, ModelFinder: Fast model selection for accurate phylogenetic estimates. *Nat. Methods* **14**, 587–589 (2017).
45. A. J. Drummond, M. A. Suchard, D. Xie, A. Rambaut, Bayesian phylogenetics with BEAUti and the BEAST 1.7. *Mol. Biol. Evol.* **29**, 1969–1973 (2012).
46. R. Lanfear, P. B. Frandsen, A. M. Wright, T. Senfeld, B. Calcott, PartitionFinder 2: New methods for selecting partitioned models of evolution for molecular and morphological phylogenetic analyses. *Mol. Biol. Evol.* **34**, 772–773 (2017).
47. R. Jong, Fossil butterflies, calibration points and the molecular clock (Lepidoptera: Papilionoidea). *Zootaxa* **4270**, 1–63 (2017).
48. M. Espeland *et al.*, A comprehensive and dated phylogenomic analysis of butterflies. *Curr. Biol.* **28**, 770–778.e5 (2018).
49. R. J. Wootton, Function, homology and terminology in insect wings. *Syst. Entomol.* **4**, 81–93 (1979).
50. M. Condamin, *Monographie du genre Bicyclus (Lepidoptera Satyridae)*, (IFAN-Dakar, Dakar, 1973).
51. M. F. Braby, Phenotypic variation in adult *Mycalesis hübner* (Lepidoptera, Nymphalidae, satyrinae) from the Australian wet-dry tropics. *J. Aust. Ent. Soc.* **33**, 327–336 (1994).
52. J. C. Roskam, P. M. Brakefield, A comparison of temperature-induced polyphenism in African *Bicyclus* butterflies from a seasonal savannah-rainforest ecotone. *Evolution* **50**, 2360–2372 (1996).
53. J. Schindelin *et al.*, Fiji: An open-source platform for biological-image analysis. *Nat. Methods* **9**, 676–682 (2012).
54. C. A. Schneider, W. S. Rasband, K. W. Eliceiri, NIH image to ImageJ: 25 years of image analysis. *Nat. Methods* **9**, 671–675 (2012).
55. H. Wickham, *ggplot2: Elegant Graphics for Data Analysis*, (Springer-Verlag, New York, 2016).
56. R Core Team, R: A Language and Environment for Statistical Computing, Version 3.6.3 (R Foundation for Statistical Computing, Vienna, Austria, 2018). [www.R-project.org/](http://www.R-project.org/).
57. A. E. Raftery, Approximate Bayes factors and accounting for model uncertainty in generalised linear models. *Biometrika* **83**, 251–266 (1996).
58. E. van Bergen *et al.*, Conserved patterns of integrated developmental plasticity in a group of polyphenic tropical butterflies. *BMC Evol. Biol.* **17**, 59 (2017).
59. R. Lenth, H. Singmann, J. Love, P. Buerkner, M. Herve, emmeans: Estimated Marginal Means, aka Least-Squares Means (R package version 1.4.3.01, 2019).